NTNU – Trondheim
Norwegian University of
Science and Technology

Seebeck and Peltier coefficients of hydrogen electrodes related to the PEMFC

Papy Zefaniya

Chemical Engineering and Biotechnology
Submission date: September 2012
Supervisor: Signe Kjelstrup, IKJ
Co-supervisor: Odne Burheim, IKJ
Kaushik Jayasayee, IKJ

Norwegian University of Science and Technology
Department of Chemistry

Thermopower of concentration cell with hydrogen electrodes related to PEMFC

Papy Mutuwa Zefaniya
Department of Chemistry
NTNU
zefaniya@stud.ntnu.no
Main supervisor: Signe Kjelstrup
Co-supervisor: Odne S. Burheim
Co-supervisor:Kaushik Kayasayee.

September 26, 2012

1 Acknowledgement

My interest for clean energy started when I first heard about the advantages of sustainable energy at the University College of Telemark in the course of Separation techniques. It further grow up in the Non-Equilibrium Thermodynamics classes of S.Kjestrup. She talked about the lost work which is of considerable amount through heat in different chemical and electrochemical systems. She further went on showing how they can be minimized through the right knowledge of entropy of the system in question, and how the lost work in heat for how it could be won back to valuable energy form. This kept on ringing in my head until I decided to pursue and learn more thermal effects and the fuel cells. In deed, fuel cell were the best candidate to learn more about, because its research field is growing and it is the most promising competitor to internal combustion engine so that our towns can be safer place to live in now and in the future.

My decision to continue Masters' degree in Chemistry was motivated by the description of the specialization course. I was first thinking that I should find a work before I could continue with my Masters degree. At the same time, I was checking, alternative option, if I would have to wait for a work for two months. I am kind of a person who likes to learn new things all the time. After reading what NTNU had to offer, I decided to go for Masters and concentrate on my Major of Studies. The start was hard and discouraging when I started my Major of studies course. But life's lesson kept me strong enough to never let it go cause every knowledge counts no matter how small you may acquire it.

My background was kind of chemical engineering with a specialization in Energy and gas Technology. This was a little bit different from Physical Chemistry. I was encouraged by my Supervisor and my co-Supervisor Odne to read many interesting books and papers which increased the intuitive meaning of what I was studying. I'm greatly thankful for what I learned verbally and by observation from Odne. He introduced me to scientific thing way and what research is. How to make my thought understood on a paper in a scientific. So many thanks to you two.

Moreover, I'm very grateful to the kindness shown by my new co-supervisor, Kaushik, who was always there to give me a hand and encouraging me in the lab when things seemed to grow hot. Also I was suprised by the friendliness of members of Kjelstrup's group. They were all willing to take in a new person in their group as part of them. Thanks to all you.

Special thanks go to Anders Lervik who introduced me to Latex. I don't forget my friend Burak Calmak who took time to recover my document at the last night before the deliverance of my work which suddenly crushed some few days before delivering it.

My Special thanks to all friends and relatives I've met in my every day life. Being far or near, you all meant something to the achievement of this work.

Finally, I Thank The Most High God for everything I went through during my period of studies at NTNU. May it seem good or bad, He always made my spirit stay strong with A great Hope to Reach Something greater One day.

Abstract

The coefficient of Thermoelectric power of hydrogen electrode as function of partial pressure has shown to be negative in accordance with the negative sign of state function of entropy with a deviation of almost half its size. The value found was $-48.8 \pm 32.2 \mu V/K$. The intercept was found to be about $666 \pm 48.7 \mu V/K$. This value of intercept can be used to determine the Peltier coefficient. The All the Seebeck coefficients were measured positive with reference to the hot electrode. On the other hand, this power is produced on the cost of absorbing the heat from the environment(heat reservoir). If this is related to electrolysis devices, this means more care should be taken on the hydrogen electrode which has an endothermic reaction to avoid the freezing of the anode electrode. In the case of fuel cell, this will mean that extra care should be taken on both Hydrogen and Oxygen electrode, since all the adsorbed heat are thrown to the other side of where reduction occurs. These heats have been defined as Peltier heats of single electrodes. Good knowledge of the magnitude of these heats will save the life of the expensive materials in fuel cell and will improve the design of thermocells which can in turn help the efficiency improvement of those cells. The temperature profile of the hydrogen electrode cell was analysed. The causes for drop in voltage were properly explained. The theory of non-equilibrium thermodynamics was adopted to explain the experiment done in this work.

Contents

List of Figures

List of Tables

2 Introduction

The heat production in a fuel cell have attracted the attention of many researchers in these recent years. The heat production in fuel cell can be very crucial for the optimization of fuel cell.

In section 3 the theory is presented followed by the experimental where the procedure of work is presented in section 4, then the results are presented in section 5 and finalised by a conclusion in section 6.

3 Theory

Thermocells are very good instruments for determining thermodynamic functions. They closely relate the Gibbs free energy, and then the entropy change of different solutions in a concentration cell to the corresponding measured amount of the electrical potential produced [1]. The thermodynamic and kinetic parameters of electrochemical reactions can thus be obtained by simultaneous measurements and analysis of heats of electrodes [2, 3, 4], electrode potential and electrical current under various conditions. This makes it easier to determine directly the entropic Peltier, and thus the reversible heats of the electrodes in a concentration cell.

Most of thermocells are heterogeneous systems. They need a rigorous theory to give a detailed description of changes taking place in them. The theory which is conveniently applicable in both laboratory and industrial scale is the theory of Non-Equilibrium thermodynamics (NET). The theory allows to obtain transport equations in a systematic way for both homogeneous and heterogeneous systems. Until recently, the extended theory of NET by Skjeltrup and Bedeaux on heterogeneous systems has shown to be more convenient to be applied to different electrochemical cells. Their theory is ordered and systematic. It accounts for the transport phenomena of surfaces and interfaces in heterogeneous systems [5, 6, 4]. It also combines the mass and energy balance with Gibbs and Nernst equations leading to entropy balance and production [7, 8]. Fuel Cells and other non-isothermal cells are examples of heterogeneous systems.

Based on the fact that their theory fits best on systems similar to the system used in this work, it is undoubtedly the best candidate tool of choice to be adapted for the description of the system in this work. (See Chap. 13 to 19 in [5]). (See also [8, 6, 4]).

3.1 System Description

The system can be subdivided into two main systems. The two reservoirs for controlling the temperature of the cell, and the cell where thermoelectrochemical reactions are occurring.

The cell is cylindrical with half cells mirror symmetric at the centre plane of the polymer electrolyte membrane. The cell system is composed of several thermodynamic subsystems which are heterogeneous. It is made of three bulk and two surfaces subsystems.
The three bulk subsystems are the anode backing(a), the cathode backing(c) and the membrane (m). The surface subsystems are the two catalytic layers (sa and sc). The membrane is a proton conducting membrane (Nafion 1110) when it is completely wet. The electrodes are identical. They are Porous Transport layers (PTL) coated with a Micro Porous Layer (MPL) and platinum catalytic layer(Pt). The cell reaction occurring at the electrode interfaces which includes a thermo-osmotic contribution can be written as:

$$\frac{1}{2}\mathrm{H_2(a)} + \mathrm{t_w H_2O(a)} \rightarrow \frac{1}{2}\mathrm{H_2(c)} + \mathrm{t_w H_2O(c)}$$

The total pressure is kept constant. While the hydrogen pressures on the two electrodes can be slightly different due to different temperatures.

The notation used Bedeaux and Kjelstrup, Chap 9, and 19 [5] will be adopted and a detailed analysis of this system using NET was well explained in the same reference including Chap.13 [5]. Only the balance conditions and transport equations will be presented in this section. Then the expression for Seebeck and Peltier coefficients which presents the basis for the experiment of this work will be derived.

Figure 1 illustrates the meaning of the notation which are adopted. The subscripts Δ refer to the two locations between which the difference is taken, s is the electrode surface, while i and o are homogeneous phases (a,m or c).

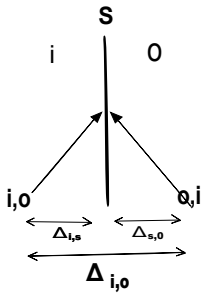

Figure 1: Notation used for transport across interfaces

3.2 Balance equations

The cell used is positioned in vertical position. The hotter side is the upper half cell and the low half cell is kept colder. If considering the vertical direction as x-direction, and the rest to be perpendicular axes, the transport problem can be restricted to one-dimensional. This is to say that there is no heat flow in perpendicular direction to x-direction transport. This energy flux in x-direction is due to charge and mass transfer.

3.2.1 Mass balances

The reaction taking place at the electrode region causes some ionic mobilities. The electrochemical reaction at Pt is given by:

$$\frac{1}{2}H_2 \rightarrow H^+ + e \tag{1}$$

At stationary state there is disappearance and production of hydrogen including a movement of water under the electro-osmotic drag and thermo-osmotic force. The transport of water and hydrogen can be related to the electric current based on the knowledge of their transport number. (See Chap.9 in [1]).
The fluxes of hydrogen gas, J_{H_2} and water, J_w, in and out membrane can be respectively given by

$$J^a_{H_2} = \frac{j}{2F} = J^c_{H_2} \tag{2}$$

$$J^{a,m}_w = J^{c,m}_w = {t_w}^m \frac{j}{F} = J_w \tag{3}$$

where t^m_w is the transference number of water in the membrane and F is a Faraday's constant. The Eq. 3 shows how water flux is balanced through the surface and through the membrane, while the flux of hydrogen stops at the surfaces.

3.2.2 Energy balance

Through the layers there is mass flow and transformation of internal energy into enthalpy. The enthalpy of hydrogen in this case is the source of the electric potential. That means the electrical potential will depend on the reference state of the enthalpy of the hydrogen.
At the anodic interface side (a,m), there is energy flux which is equal to:

$$J_u = {J_q}^{'a,m} + J_{H_2}{H_{H_2}}^{a,m} + J_w{H_w}^{a,m} + j\phi^{a,m} \tag{4}$$

This energy is constant through all layers and interfaces. Therefore, a similar equation as Eq. 4 will be expected in the cathode side at the interface with the membrane in MPL (c,m). The H_i stands for partial molar enthalpy of i component. In the membrane-anode interface, the energy flux si given as

$$J_u = {J_q}^{'m,a} + J_w{H_w}^{m,a} + j\phi^{m,a} \tag{5}$$

A corresponding energy flux as Eq. 5 will also be found near the membrane-cathode-side(m,c).

3.3 Transport equations

In this section the transport equations in the layers within the cell are derived. Transport per unit area in one direction across the membrane of the cell. The frame of reference for the fluxes is the static surface of Nafion.

3.3.1 The PTLs and MPLs

In the electronic conducting layers there are fluxes of mass, charge and heat which in turn contribute to the entropy production in those layers. Since detailed conditions of water at the surface are not very well known, a standard simplification for resolving this problem will be to assume that there is equilibrium of water across the surfaces between the PTL-PML and membrane(ref to Eq. 3). Hence, only two fluxes remain and which contribute to the entropy production.
The fluxes-forces relations in these layers are given by

$$J_q{}'^a = -\lambda^a \frac{dT}{dx} + \pi^a \frac{j}{F} \tag{6}$$

$$\frac{\phi}{dx} = -\frac{\pi}{TF}\frac{dT}{dx} - r^a j \tag{7}$$

where λ^a is the thermal conductivity of graphite-matrix, r^a is the electric resistivity of graphite matrix, and π^a is the Peltier heat of electronic conductor which can be quantified as the transported entropy carried by positive charges times the average temperature of the medium through which is transported. This Peltier heat of the electronic conductor is given by

$$\pi^a = TS_e{}^* \tag{8}$$

where $S_e{}^*$ is the transported entropy of electron in J/molK and T is the average temperature of the cell in K. The practical meaning of Peltier heats and transported entropy will be given vide infra.

3.3.2 The electrode region on the anode side

The contributions to entropy production in this layer is the same as in section 3.3.1. The additional contribution due to electrochemical reaction taking place at the surface is given by Eq. 1. The Peltier term in this case takes into consideration the molar entropy liberated when a mole of hydrogen reacts onto the surface of the catalytic layer. The formed goes through the membrane carrying a molecule of water which is termed as electro-osmotic drag. On adding the Peltier entropy intake from the heat reservoir to the net increment in entropy of the electrode region, the following equation is obtained:

$$\frac{\pi^a}{T} = \frac{1}{2}S_{H_2} + S_e{}^* \tag{9}$$

where S_{H_2} is the molar entropy liberated at the anode electrode. The heat fluxes in and out of the surface layer with contribution from Peltier heats can thus be written as:

$$J_q{}'^{a,m} = -\lambda^{as}\Delta_{a,as}T + \pi^a \frac{j}{F} \tag{10}$$

$$J_q{}'^{m,a} = -\lambda^{ma}\Delta_{as,m}T + \pi^m \frac{j}{F} \tag{11}$$

where π^m is the Peltier heat which is transported into the membrane and it is given by :

$$\pi^m = T\left(S_{H^+}{}^* - t_w{}^m S_w{}^m\right) \tag{12}$$

where $S_w{}^m$ is the partial molar entropy of water in the membrane, and $S_{H^+}{}^*$ is the transported entropy of the protons into the membrane.

3.3.3 Transport in the Membrane

The entropy production in the membrane has contributions from heat, water and proton fluxes. The electric potential arising in the membrane can thus be given by:

$$\frac{d\phi}{dx} = -\frac{1}{TF}(\pi^m - t_w q^{*m})\frac{dT}{dx} + r^a j \tag{13}$$

where q^{*m} is water heat of transfer. This is the heat which must be transferred to the surrounding due to increase in transported entropy in membrane when 1 mole of water migrate into the membrane(ref. Chap.02.p37 in [9]). The heat of transfer at the water equilibrium condition in the membrane $(d\mu_w = 0)$ is given by:

$$q^{*,m} = -TS_w{}^m \tag{14}$$

At the beginning of the experiment (t=0), just when a temperature gradient starts to establish in the membrane, the flux of water is normally zero. The stationary state develops as a constant temperature difference relaxes at t=∞. The direction of water due to heat flux is normally specified by the property of the membrane [10, 11]. The transport equations in the membrane are given by three set of equations:

$$J_q{}'^m = -\lambda^m \frac{dT}{dx} + q^{*,m}\left(J_w - tw\frac{j}{F}\right) + \pi^m \frac{j}{F} \tag{15}$$

$$J_w = -\frac{q^{*,m} c_w D_w}{RT^2}\frac{dT}{dx} + -\frac{c_w D_w}{RT}\frac{d\mu_{w,T}}{dx} + t_w \frac{j}{F} \tag{16}$$

$$\frac{d\phi}{dx} = -\frac{\pi^m}{TF}\frac{dT}{dx} + \frac{t_w}{F}\frac{d\mu_{w,T}}{dx} + r^m j \tag{17}$$

where λ^m is the thermal conductivity of the membrane, r^m, D_w, c_w and R are the electric resistivity, diffusion coefficient of water, the concentration of water and the gas constant respectively. When the mass balance is considered as in Eq.(3), the Eq.(16) reduces to the condition for Soret equilibrium:

$$\frac{d\mu_{w,T}}{dx} = -\frac{q^{*,m}}{T}\frac{dT}{dx} \tag{18}$$

where the relation $d\mu_T = SdT + d\mu$ leads to the Eq.(14).

To get the potential difference across the membrane, the Eq.(17) has to be integrated across the membrane thickness. When assuming that the current crossing the membrane is very insignificant (j=0), only the temperature gradient remains as the cause for potential difference. This is the called the Seebeck effect. The Eq.(17) reduces to :

$$\Delta_m \phi = -\frac{1}{F}\left[S_{H^+}{}^* - t_w\left(S_w{}^m + \frac{q^{*,m}}{T}\right)\right](T^{m,c} - T^{m,a}) \tag{19}$$

It should be noted that this equation describes the situation after steady state. The temperatures at the interfaces are considered to be equal. Because the thermocouples which are used to measure the temperatures at the interfaces are thicker than the thickness of the surface electrodes.

3.3.4 The surface and the transport layer on cathode side

Since the electrodes are similar, one can only expect the same amount of heat on the other electrode. The reason for this is, there is no work which is needed to transfer unit charge through the system because the two electrodes are symmetric and identical. This means $dW = 0$ because the amount of heat absorbed into the anode region from the heat reservoir, [12] is the same amount removed from the cathode region. By considering the first law of thermodynamics, only the work term remaining is the one due to heat. This heat is transformed into electric work du to Seebeck effects.

3.4 The Seebeck coefficient

The Seebeck coefficient can be measured in two ways. It can be measured in initial condition i.e, right after the establishment of temperature gradient in the system [9, 13]. The terminology of quasi stationary state (or steady state at t=n) will be adopted to avoid the confusion with the initial condition which refers to t=0, before the temperature gradient has been established in the cell. The stationary state will be used when talking about the Soret equilibrium. The cell voltage is the sum of all voltage contribution from all layers from the anode to cathode when the current is negligibly small ($j \approx 0$):

$$\Delta_{a,c}\phi = \Delta_a \phi + \Delta_{a,m}\phi + \Delta_m \phi + \Delta_{m,c}\phi + \Delta_c \phi \tag{20}$$

The Seebeck coefficient is found by dividing this voltage by the temperature difference between the electrodes. Initially, when temperature difference is zero, ($\Delta_{sa,sc}T = 0$), t also is considered to be zero, ($t = 0$). At this moment, the Seebeck coefficient fluctuates between zero and infinite. The reason for this fluctuation is difficulty to restrict the value of either Seebeck coefficient or temperature difference to zero due to systematic reasons. As a consequence a value with noises can be observed due to $\frac{0\pm\#}{0\pm1}$ μV/K.The # symbolize avalue at which the

Seebeck coefficient is. When the temperature difference reaches steady state (quasi state) at t=n minutes, the following expression for Seebeck coefficient is obtained:

$$\left(\frac{\Delta_{a,c}\phi}{\Delta_{sa,sc}T}\right)_{j\approx 0,t=n} = \left((\frac{1}{2}S_{H_2} + {S_e}^*) - {S_{H^+}}^* + t_w {S_w}^a\right)\frac{1}{F} \tag{21}$$

where n is the time from relaxation time to infinity ∞. After the temperature has relaxed, theoretically it takes some times due to slow movement of water to equilibrate in the membrane which is subjected to temperature gradient. When the Soret equilibrium has established,(see Eq. 18), the following equation is obtained:

$$\left(\frac{\Delta_{a,c}\phi}{\Delta_{sa,sc}T}\right)_{j\approx 0,t=\infty} = \left((\frac{1}{2}S_{H_2} + {S_e}^*) - {S_{H^+}}^* + t_w({S_w}^a + {q^*}^{,m}/T)\right)\frac{1}{F} \tag{22}$$

With by substituting the heat of transfer term by the partial molar entropy of water in the membrane from the relation in Eq. 14, the Eq. 22 reduces to

$$\left(\frac{\Delta_{a,c}\phi}{\Delta_{sa,sc}T}\right)_{j\approx 0,t=\infty} = \left((\frac{1}{2}S_{H_2} + {S_e}^*) - {S_{H^+}}^* + t_w({S_w}^a + {q^*}^{,m}/T)\right)\frac{1}{F} \tag{23}$$

The measurement of soret coefficient is very lengthy and cumbersome to achieve in a short period of time. In a dilute solution like the one in this work, it requires very high precision in voltage measurement to account for the difference between the "quasi state voltage"(called initial voltage in literatures [9, 14, 15, 13]) and stationary state voltage. It can take more than 24 hours before the Soret equilibrium establishes. Most of the time, the magnitude of Soret is very small compared to that found at quasi state, i.e right after the temperature has relaxed completely. Based on this reasoning, it will be assumed that the contribution of soret effect is inconsequential on the measured Seebeck coefficient in this work. It will thus be assumed that the steady state is reached when the temperature is reached.

3.5 Peltier coefficient

Originally the Peltier effect was observed in metallic conductors.The effect can cause cooling or heating in the junctions of the conductors. When the current passes there will be a rise of temperature due to Joule heating causing additional temperature changes at the junctions. These Peltier temperatures are of opposite signs at the two junctions, and they are reversible by reversing the direction of the current. Similarly, the Peltier heats can be analysed in the electrochemical systems where chemical change occurs when there is a current flow.

The cooling and heating effect can be substantial in electrochemical cells. In the present concentration cell, where the two electrodes are similar, the electrode entropy changes are reversible, i.e equal but with opposite signs. This can lead to cooling of one part and heating of the other. These temperature jumps can be compensated by adding heat from an external reservoir to one junction and removing an equal quantity of heat from the other. That is to say one half cell can be constantly heated while the other is constantly cooled.

At constant temperature and constant pressure, the heat entering the electrode divided by the temperature is called the single electrode Peltier entropy. This entropy can easily be related to the Seebeck coefficient. Its magnitude is equal to the sum of the net increment entropy change of the electrode and the transported entropy.

As it was stated earlier, the heat absorbed at the electrode can be directly related to the electrical work produced by the electrode by this relation:

$$\frac{\pi_{H_2}}{T}dT = -Fd\phi \tag{24}$$

where $\frac{\pi_{H_2}}{T}$ can be related to Eq. 23 at stationary state and get the expression of Petier coefficient as function of molar entropies and transported entropies as

$$\left(\frac{\pi^a}{T}\right)_{j\approx 0,t=n} = \left((\frac{1}{2}S_{H_2} + {S_e}^*) - {S_{H^+}}^* + t_w({S_w}^a + {q^*}^{,m}/T)\right)\frac{1}{F} \tag{25}$$

Since the electrodes are similar, the Peltier coefficient of cathode will be equal to the negative Peltier coefficient of anode such as:

$$\pi^c = -\pi^a \tag{26}$$

The famous analysis of variance, ANOVA, and analysis of dispersion of errors were used to evaluate the exactitude of the derived results.The variance equation is given by;

$$\sigma_f{}^2 = \frac{1}{n-1}\sum_{i=1}^{n}(f_i - f)^2 \tag{27}$$

and the formula for transmission of errors is

$$\{\sigma_f\}^2 = \sum_{i=1}^{n}\left(\frac{\partial f}{\partial x_i}\sigma_{x_i}\right)^2 \tag{28}$$

where f is the function of several variables and σ_{x_i} is the standard deviation of variable x_i.
The results in this work are presented with double standard deviation based on Eq. 27. Finally, the linear regression was achieved by using the least-squares method and Excel was used to perform the calculations.

4 Experimental

The cell used for Seebeck coefficient measurements was reported earlier by Vie Et al.[16]. It was cylindrical with half-cells in symmetric mirror at the centre plane of a wet polymer electrolyte membrane. The thickness of the membrane was 873µm thick. A mechanical pressure of around 9.3 bar was applied to the half cells to achieve a desirable contact between the diffusion layers, electrodes and the three Nafion 1110 membranes. Four thermocouples of K type were inserted in the cell as illustrated in Fig. 2 and their thickness varied with $\pm$ 0.25 mm. The membrane was sandwiched between two identical catalytic-coated porous transport layer.

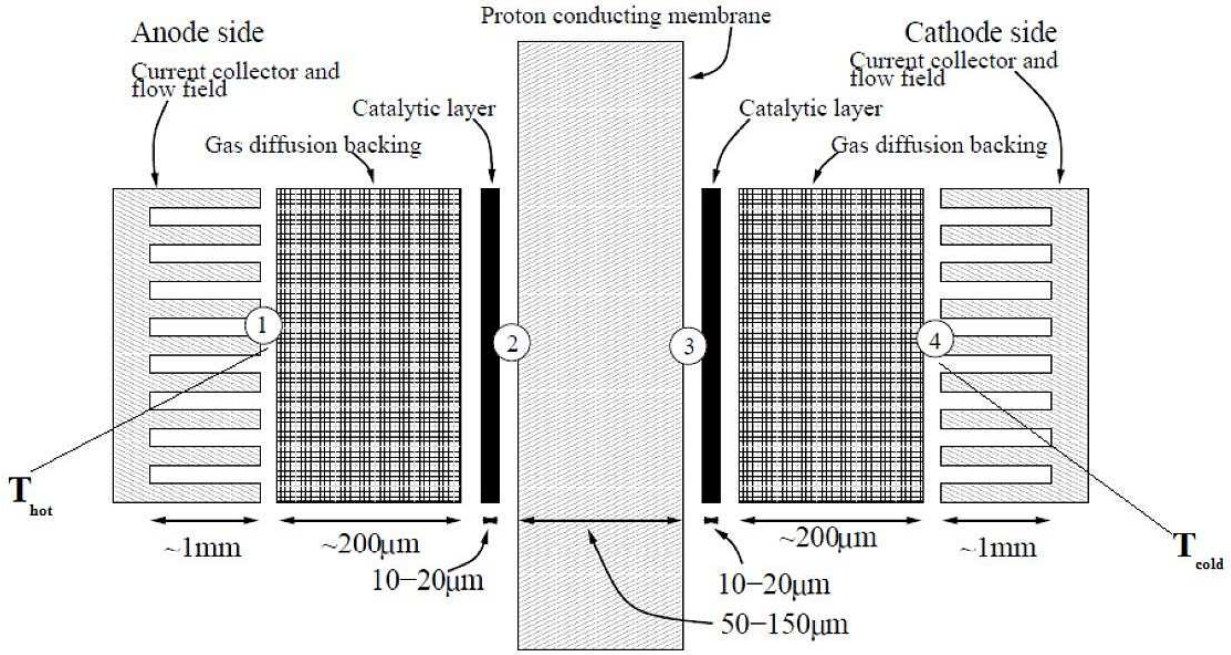

Figure 2: A sketch of the cell showing the positing of thermocouples. The wires measuring the open circuit voltage were situated around points ② and ③ respectively, and four k-type thermocouples were put in locations ① to ④ to measure the temperature

Platinum catalytic sides were facing each side of membrane. Two Pt-wires were also inserted in both side of membrane near point ② and ③ to measure the voltage across the membrane. The two Pt-wires were insulated

with a small hose reinforced with PTFE. Their end points were left exposed to about 1 mm long and 0.2 mm thick. Almost a total of about 8 mm long Pt-wire (when measuring from the edges of the active area) was inserted between the membrane and the catalytic layer with a shield layer making a total thickness of 0.3 mm

After assembling the cell, a temperature difference across the cell was imposed by encapsulating each half cell in custom-made heating jackets. Two heaters were streaming water through each jacket to maintain a constant temperature inside the cell. Two separated water baths were used for this purpose.

The compaction pressure inside the cell was attained by correlating the pressure read on the manometer of nitrogen tank to the pressure inside the cell. The contact area where nitrogen pressure was applied was not equal to the of the cylinder inside the cell. The pressures were related by the simple relation as follow:

$$\frac{P_{in}}{P_{N_2}} = \frac{A_{ext}}{A_{in}} \tag{29}$$

where P_{in} is the compaction pressure inside the cell, P_{N_2} is the external compaction pressure read from nitrogen tank, A_{ext} is the external surface area on which nitrogen pressure is applied, and A_{in} is the active surface area inside the cell. The active area was about 4.9 cm^2.

4.1 Procedure

Each half cell was now encapsulated with custom-made heating jackets, allowing a temperature difference across the cell membrane. Water from heating and cooling source were streaming through each jacket, maintaining a constant temperature inside the jacket and in the half cell. Two separate water baths were used for this purpose.

Calibration of thermocouples was done in water with ice, giving a variation of less than $\pm 0.1^{\circ}$C. A verification of temperature measurement was also performed prio to experiment start by keeping uniform temperature on both sides of the membrane, and compare the readings to that shown in the heat source. This was a confirmation of uniformity of temperature measurements at the corresponding location of thermocouples. The position of the thermocouples are shown in Figure 2.

One to four Nafion 1110 were used as membrane, to maintain a stable temperature gradient with different sizes of membranes. The membranes were sandwiched between two catalyst-coated porous transport layers (E-TEK single sided coating, 0.8 mg/cm^2), identical on the two sides of the membrane; the catalyst facing the membrane. The cell potential was measured between the current collector plates, with electronic connection via carbon fibres to the catalytic layer.

The hydrogen gas (99.99% purity) was humidified in external humidifiers (with distilled water), which were kept at constant temperature, so that the gas entering the cell was slightly supersaturated with vapour. Some liquid water would therefore always be present. The gases streamed through the cell very slowly at about 0.02 to 0.04 l/s, keeping open the path for hydrogen to the active site. The feeding channels' depth and width were 0.5 mm and 1.0 mm, respectively.

The concentration cell used, was made of similar components as that of PEMFC. Therefore, all measures taken for keeping good operation and performance of PEMFC applies in very great degree to this experiment as well. Except that an oxygen electrode is not used here. By simple standard notation, the concentration cell used here can be denoted as:

$$(\mathrm{Pt,C})\mathrm{H_2}(\mathrm{p^a,T^a}) \mid \mathrm{H_2O}(\mathrm{p_w,T^a}) \mid^{\mathrm{m}} \mid \mathrm{H_2}(\mathrm{p^c,T^c}),\mathrm{H_2O}(\mathrm{p_w,T^c}) \mid (\mathrm{Pt,C})$$

4.1.1 Humidifiers and temperature

One bubble humidifier was used to humidify the H_2-gas externally before entering the cell. The detail technical description of this humidifier is found in the reference [17]. The temperature in the humidifier was controlled by a temperature controller. The temperature was fluctuating above the set-point within ± 2 K before stabilising at the set-point in the humidifier. The cooling down control of humidifier was taking some time since the system was depending on cooling effect from the surrounding. The duration of adjustment was depending of the initial starting temperature. Cooling down to the set-point was time consuming and tedious. A considerable amount of water was ensured to be above half level of the bottle in the humidifier. This is in accordance with the findings of Vasu et al. [18]. Vasu et. have found that water level in the humidifier has an impact on the

relative humidity of H_2 at low flow rate, but not at higher flow rates. They found that with a water level higher than half of the bottle in the humidifier, would be enough for hydrogen molecule to reach relative humidity of between 93% and 96% depending also on operating temperature.

After checking for any leakage, the controller heater for humidifier was set on, then the gas stream was allowed to flow in the cell entering by the hotter half cell, then circulated in the colder half cell and went out. The had thus 1 gas inlet and one gas outlet to avoid possible difference in pressure in the two half cells. One gas pressure was kept throughout one experiment. Four different pressures were used for the measurement of the Seebeck coefficient (0.05 bar, 0.25 bar, 0.5 bar, 0.75 bar, and 1 bar) and two more were attempted (1.5 bar and 2 bar.

First, the humidifiers temperature was adjusted 5 K above the temperature measured in the hotter bath. Then a constant temperature gradient was imposed to the cell while keeping the average temperature of the cell constant. Every time a new temperature difference was set, a humidification temperature was also changed. 4 to 5 different temperature differences were imposed while keeping same average temperatures. The humidification temperature was increased by the operator each time a new target of temperature difference was adjusted.The ratio of temperature difference over the membranes and in gas channels was compared to the ratio of membrane resistance over the total materials' thermal resistance to quickly check the degree of humidification state of the cell. The values were taken from [19]

4.1.2 Controllers

At the beginning of the experiment, the system was mostly controlled manually. Then it was slowly improved throughout the course of the work by equipping the system with a flow-controller and needle valves to maintain constant gas flow into the cell. The gas was made to use one gas inlet and one outlet to avoid unequal flow rate in the two half cells since there was only one flow controller available.

Finally, an experiment with reduced partial pressure of hydrogen mixed with helium was conducted by changing temperature gradient together with humidification temperature in the humidifiers at a constant average temperature. The pressure above 1bar was obtained by the help of application of back pressure. The pressures used this report were 0.05, 0.25, 0.5, 0.75, 1 and 1.5 bar respectively. Two cell average temperatures were used; 40 and 60 °C. The relaxation time of temperature was obtained between 15 min and 60 min (depending on the size of temperature difference one wants to achieve) See Fig 3.

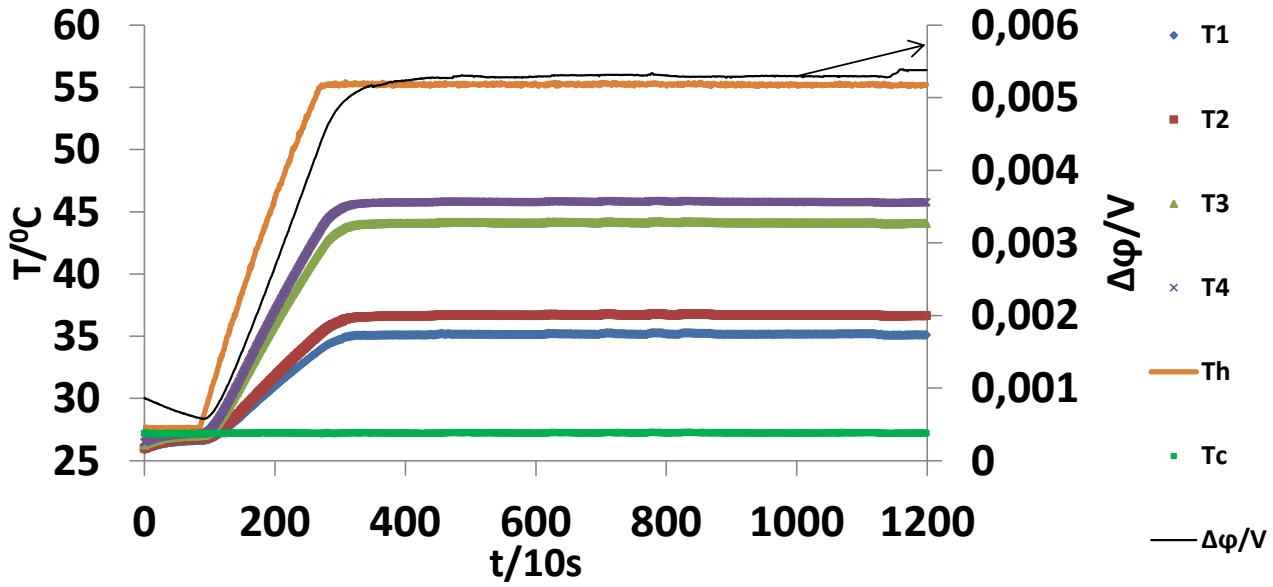

Figure 3: A graph showing the experiment with the recorded temperatures in the baths and in the cell. The temperature in the cold bath was held constant from the start of the experiment in question until the end as shown in the lowest line. The hotter bath was allowed to increase, in this case, up to 55 °C. The average temperature in the cell and in the baths was almost equal with slight difference of 1 °C which can be attributed to dissipation in the surrounding.

5 Results and Discussion

5.1 Temperature measurements

In this section the results of measured temperatures in the local and whole system are presented and discussed in the view of the temperature gradient in a PEM fuel cell. The presented results are measured from direct application of heat on each half cell to establish local equilibrium in the four different subsystems of the concentration cell made of PTLs coated with platinum on each side of the membranes.

Four different thicknesses, as described in the experimental section, were used to verify the temperature differences between the contact surfaces and gas channels. A general discussion concerning all of them will be included in this section.

Since the cell was used as a thermocell, it was possible to get accurate reversible heat effect in all the four parts and achieve local equilibrium in each sub-part. See fig: 4.

The main factors influencing the stability of measured temperature in the four different parts in the cell were humidity,water in the baths and the state of the water in gas channels. Thus, it was important to start by looking at those three factors in detail in order to understand the state and impact of temperature on the measured voltage in the cell.

5.1.1 Temperature in the reservoirs

The stability of the temperature in the cell was controlled by help of two water baths/reservoirs. One reservoir was used for cooling and the other one for heating. A coil tube was circulating cold water from the tap to ensure that the colder reservoir remained stable. At a higher starting temperature, the water tap was stopped to avoid further cooling of the intended temperature. In the beginning, the temperature in the bath was observed by bare eye on the indicator which was on the thermomixer. This could not give a reliable temperature value which could be reported since their sensors were not calibrated. Then two thermocouples of K-type were inserted in both reservoirs and recorded the temperature in the computer as time went by.

The stationary state was attained after 9 m 50 min for the lowest and highest temperatures respectively. This is an indication of good thermal transferability. The double standard deviation of each temperature mea-

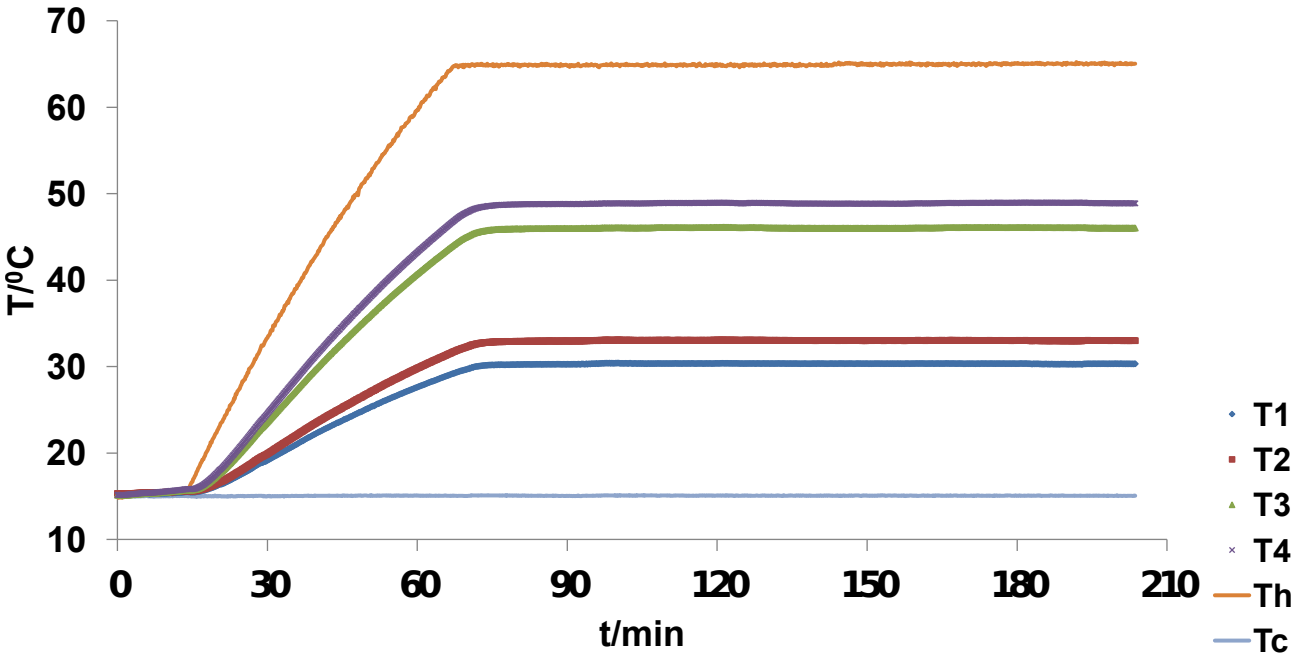

Figure 4: Typical measured temperature in the bath and in the concentration cell. T_h and T_c stand for temperature in hot and cold baths respectively. Each experiment was started at isothermal condition. The position of the thermocouples are shown in Fig. 2

surement in each reservoir was measured to be within the margin of $\pm 0.4\%$ of the measured temperature at steady state. The average temperature in the reservoirs(both of them together) was 40 ± 1 °C. It was ensured that the second law of thermodynamics between the reservoirs and the cell to be rea for a better comparison study of phenomenon taking place in the cell. That is, the entropy change in the reservoirs plus the entropy

change in the cell should give zero so that global thermal equilibrium could be held between the two systems. [20]. The 1 °C was necessary to compensate the dissipated heat between the distance of the reservoirs and the cell due to non-isolated hoses in use. Fig 4 presents a typical result for measurement of temperature in the reservoir from the initial state to the stable state. The figure shows the direct impact of the heat transfer from the reservoirs to the cell. The time for reaching quasi steady state in the cell wasn't far from the steady state time in the baths. Only the temperature in hotter reservoir was increased, while forcing the colder reservoir to stay at the same initial temperature. The starting of the experiment with isothermal state was important for the reason of comparison between the initial state and the steady state. Nevertheless, it should be noted that at this initial state the average temperature was different from that at steady state. When two entropy changes of a system are to be compared, the temperature should at least be equal depending on the intention of comparison. The initial temperatures in both reservoirs were around 15 ± 1 °C and the stationary state temperatures were 64.9 ± 0.2 °C and 15.06 ± 0.04 °C for hot and cold reservoir respectively. To attain this accuracy in the colder bath, it was necessary to have constant circulation of a considerable amount of cold water around the cathode half cell so that a considerable amount of heat flux (from hotter side to the colder side) could be hampered at steady state without causing change of temperature in the cooler bath. Thus, the same average temperature in the cell was attained as in the baths.

5.1.2 Local temperature measurements

Temperature gradient, as the main driving force here, dictates the direction of proton and water movement in and out of the membrane. The stability of temperature measurement in cell was reached with a variation of $\pm$ 0.1 °C in stationary state. The quasi-stationary state of temperatures depends on the initial temperature and the intended temperature. This was attained after 15 min to 55 min for the lowest and highest temperatures respectively. Figure 4 and 1 show the typical temperature measurement in the cell. More measurements are found in the appendix. These results and the others show some variation in the temperature difference between the temperature in the gas channels and that in the interfaces sites. The variations can be explained in two ways. Thermocouple sizes are bigger than the size of the active catalytic layer, which implies the uncertainty of the exact measuring location. The measuring location may be at a different location such as within the PTL-matrix instead of the interface. See Fig. 5.

To see whether this was the case of what happened in the cell of the present work, a close look at variations in temperature difference between the two sides of the porous transport layer (PTL) was made at different physical conditions (number of membranes: from 1 to four). One temperature difference was randomly chosen and investigated at different conditions(membrane thickness and when the cell was re-assembled). The remarkable thing is that, in most of the cases when the cell was re-assembled, and try to repeat the same experiment at same operating conditions, the results were not directly repeating. Temperature difference over PTLs, ΔT_m, was changing giving rise to different temperature differenceover the membrane, ΔT_m. Thus, the ratio between $\Delta T_m$and temperature differencein channels, ΔT_{ch}, showed to be varying as well. (See Table 1). This could increase drastically the variation of the Seebeck coefficient as it will be made clear in section 5.3

In fact, the shape and size of the thermocouples will not only find their room in the matrix of PTL, but, can result in destroying them and making remarkable holes in them. This may result into heat leakage into the interface making the affected area either a prone to quick evaporation or flooding which can a decrease of gas permeability to the active site (if sudden considerable amount of water came in liquid form) or can simply cause uneven hydration in the membrane. [21]. The other point to consider here is the fact that the gas coming directly to the membrane surface without passing through the PTL-matrix, will miss the early adsorption stages which are important for hydrogen before reaching the active site of Pt. [5]. The other source of variation in temperature may be the presence of liquid water in the gas channels in hotter or cooler half-cell. From this point of view, it's clear that the morphological aspect of PTL is crucial when temperature and the voltage of the cell is to be measured accurately. Hence, it can be misleading to "solely" base the analytic state of humidification on the measured ratio, $\frac{\Delta T_m}{\Delta T_{ch}}$, if one does not consider the impact of the thermocouples' location PLT matrix.

The good news is that these variations are very small, and their corresponding differences are smaller compared to the temperature difference over the membranes. Their uncertainty does not affect the measured voltage. The voltage becomes affected by other factors accompanied by the fatigue inflicted on the PTL-MP-layers. Moreover, when the ratio f_{ratio} is close the calculated one, one can assume less damage on the porous layers. -Though this is not a guaranty-. Otherwise, all experiments should be conducted under the same

Table 1: Local temperature variations and the impact of thermocouples size on the temperature differences and the estimated Seebeck coefficient. The small variations have an impact on the measured temperature difference on the membrane, since the reference points changes every time a cell is opened due to the stresses and strains inflicted by compaction pressure and the size of thermocouples.ΔT_c= the temperature difference over the PTL on the cold half cell, and ΔT_h= the temperature difference over the PTL on the hot half cell. f_{ratio} is the ratio between ΔT_m and ΔT_{ch}. All these results were performed at 1 bar. The compaction pressure was around 9.3 bar

n	$Cal_{R-ratio}$	Variables	Parallel1	Parallel2	Parallel3
1		ΔT_c/K	1.76 ± 0.17	2.31 ± 0.22	2.24 ± 0.18
		ΔT_h/K	2.02 ± 0.10	2.29 ± 0.16	2.01 ± 0.11
		ΔT_m/K	4.68 ± 0.05	5.75 ± 0.10	4.61 ± 0.04
		$\Delta\phi$/mV	2.88 ± 0.16	8.04 ± 0.4	3.39 ± 0.09
		$\frac{\Delta T_m}{\Delta T_{ch}}$	0.553 ± 0.007	0.56 ± 0.013	0.52 ± 0.006
		$\frac{\Delta\phi}{\Delta T_m}$ /mV/K	0.61 ± 0.034	1.39 ± 0.09	0.72 ± 0.06
		Total Seeb.coeff /mV/K	0.68 ± 0.20	1.64 ± 0.48	0.68 ± 0.02
		Total f_{ratio}			
2		ΔT_c/K	2.32 ± 0.11	2.17 ± 0.09	
		ΔT_h/K	3.09 ± 0.12	2.95 ± 0.07	
		ΔT_m/K	8.53 ± 0.06	8.69 ± 0.05	
		$\Delta\phi$/mV	5.44 ± 0.05	5.69 ± 0.15	
		$\frac{\Delta T_m}{\Delta T_{ch}}$	0.612 ± 0.004	0.629 ± 0.004	
		$\frac{\Delta\phi}{\Delta T_m}$ /mV/K	0.638 ± 0.007	0.654 ± 0.017	
		Total Seeb.coeff /mV/K	0.63 ± 0.04	0.61 ± 0.07	
		Total f_{ratio}			
3		ΔT_c /K	0.71 ± 0.17	1.43 ± 0.07	2.31 ± 0.10
		ΔT_h/K	1.18 ± 0.19	2.23 ± 0.06	2.28 ± 0.08
		ΔT_m/K	6.70 ± 0.09	10.31 ± 0.03	10.78 ± 0.04
		$\Delta\phi$/mV	7.93 ± 0.19	5.99 ± 0.07	6.93 ± 0.30
		$\frac{\Delta T_m}{\Delta T_{ch}}$	0.78 ± 0.01	0.738 ± 0.002	0.701 ± 0.004
		$\frac{\Delta\phi}{\Delta T_m}$ /mV/K	1.18 ± 0.04	0.581 ± 0.006	0.664 ± 0.027
		Total Seeb.coeff /mV/K	1.19 ± 0.03	0.611 ± 0.065	0.612 ± 0.038
		Total ,f_{ratio}			
4		ΔT_c /K	2.07 ± 0.12	1.48 ± 0.15	1.46 ± 0.36
		ΔT_h /K	0.73 ± 0.10	1.09 ± 0.13	2.26 ± 0.16
		ΔT_m/K	12.46 ± 0.03	14.21 ± 0.13	10.36 ± 0.13
		$\Delta\phi$/mV	7.27 ± 0.11	7.69 ± 0.14	7.21 ± 0.12
		$\frac{\Delta T_m}{\Delta T_{ch}}$	0.816 ± 0.003	0.847 ± 0.006	0.735 ± 0.002
		$\frac{\Delta\phi}{\Delta T_m}$ /mV/K	0.584 ± 0.009	0.541 ± 0.008	0.696 ± 0.007
		Total Seeb.coeff /mV/K	0.594 ± 0.003	0.517 ± 0.021	0.754 ± 0.056
		Total f_{ratio}			

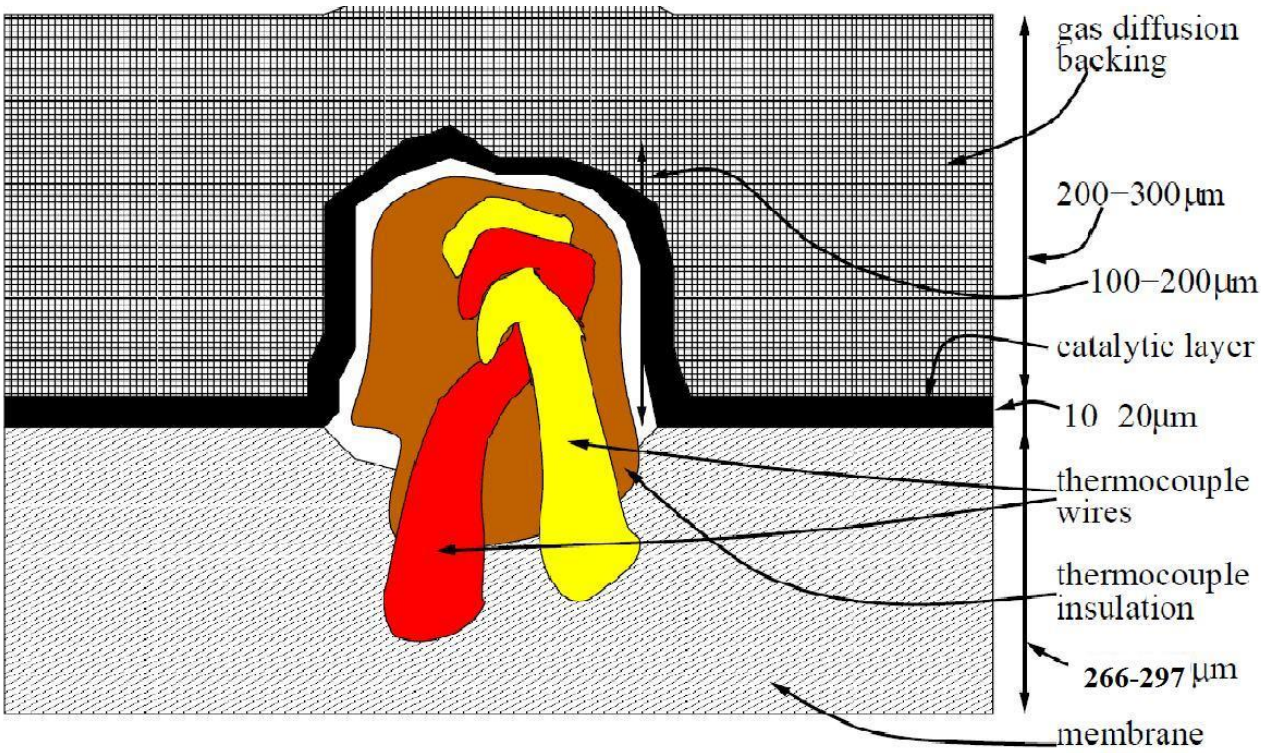

Figure 5: A sketch of a probable location of a thermocouple between the membrane and the active site. The other components which are more flexible gives room to the thermocouples.The sketch was taken from [17] and re-edited to fit the scaling size of the membrane used in the present work.

operation conditions(referring to the physical state of the system) so that the results can be reproducible, -which can difficult if the cell is filled with thermocouples between their components.

5.1.3 Cell Temperature profile

Fig. 6 shows the typical temperature profile of the concentration cell with hydrogen electrode. The temperature in the anode electrode (where electrons) are produced is higher than in the cathode electrode. The electrode surface is assumed to have a uniform temperature because of its small size. The temperature decreases along the vertical axes. And the cathode is held at a lower temperature. The heat flow in x-axes is equal. It is a sign of local equilibrium within each layer and that the voltage is measured at the vicinity of same temperature measuring point. See Figure 7 and Table 2. Two thermocouples were inserted in each gas channel, and 3 between membrane and electrodes on each side of the membrane. These results also showed as discussed above, no big distinct in vertical axes of a PTL, and uniformity in horizontal plane of the measuring plane. When a thermocouple is carelessly inserted, it can found itself measuring at the edges of electrode as the case of the light brown in the graph shows. The dropping black line is the voltage drop probably due to damaged PTL, which reduces drastically the voltage up to 100 µV. The first blue line can be the proof to this. As heat leaks through the PLT by this thermocouple,the temperature at this point increases up to the point the steady state is reached, then it falls down where the temperature relaxes. Nevertheless, the voltage continues to decrease because the flooding might be high and a great remaining part of active site might be covered by the number of thermocouples

Table 2: Measured temperatures in different locations in horizontal plane over the membranes and PTL. T_h and T_c are the temperatures in the hot and cold reservoirs. The gradual numbering of temperatures goes from lowest temperature in the cold half cell(cathode) to the hotter half cell. Two thermocouples were sat in the gas channels PTL contacts and three on each side of membrane. Three Nafion-1110 membranes were used at 1bar in this experiment.

T_1/°C	T_2 /°C	T_3/°C	T_4/°C	T_5/°C	T_6/°C	T_7 /°C	T_8 /°C	T_9 /°C	T_{10} /°C	T_h /°C	T_c/°C
32.35 ± 0.35	34.24 ± 0.11	34.36 ± 0.16	34.50 ± 0.10	34.65 ± 0.24	45.34 ± 0.13	45.46 ± 0.99	37.50 ± 0.16	46.4 ± 0.3	47.7 ± 0.3	60.0 ± 0.15	19.8 ± 0.1

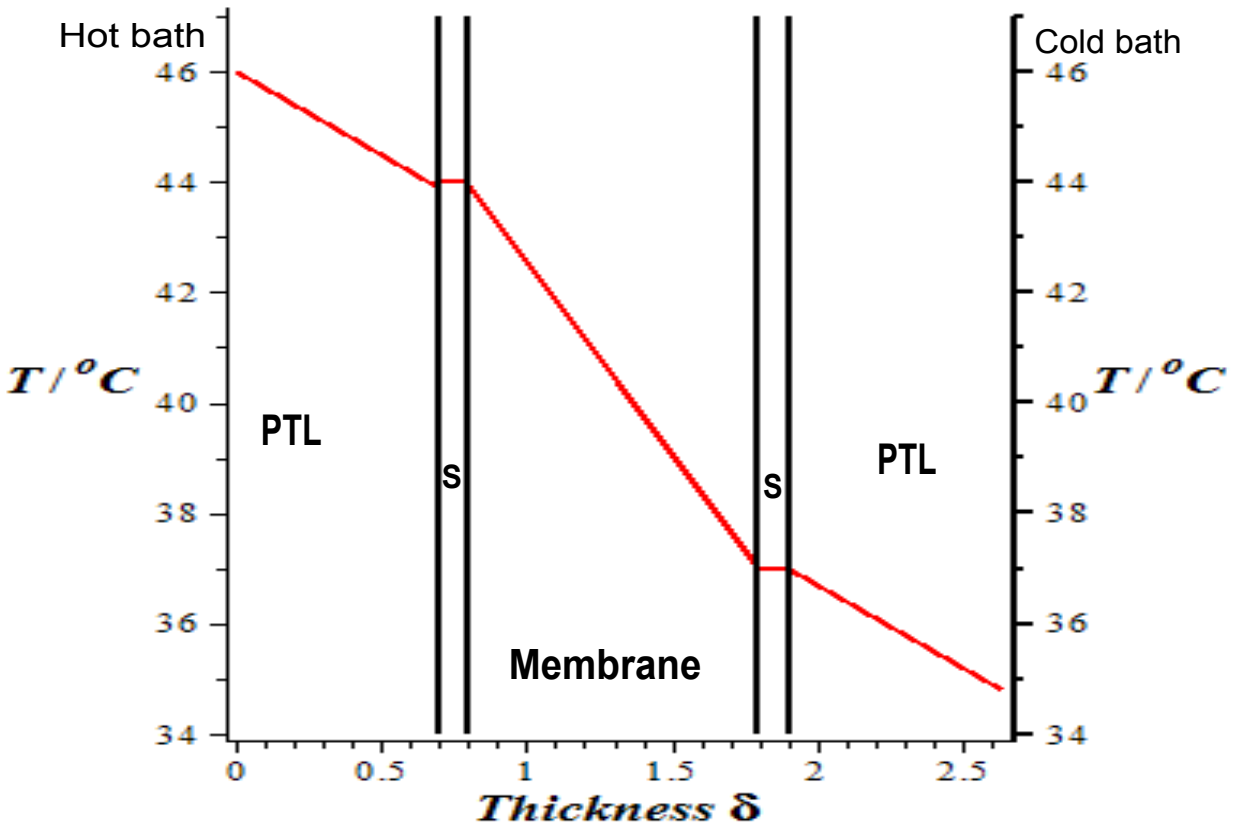

Figure 6: A typical cell temperature profile. The scaling in x-axes do not relate to actual dimensions of the components.

5.1.4 Concluding remarks on the measured temperatures

Thermal study of fuel cells is becoming more and more crucial for the optimization of PEM FC design. Exact knowledge of thermal properties of different components in the fuel cell can help modellers to easily design a fuel cell exempt of drought and flooding which are one of challenges in PEM FC. Several authors [16, 22, 23, 24] have tried to look at this issue by looking at the temperature distribution in the cell using different techniques when current flows in the cell. Their findings (and others not mentioned in this work) are the proofs of unequal distribution of heats in the PEMFC under operation [2, 25]. Motivated by the same spirit, O.Burheim,et al. [19, 26] conducted a detailed investigations on the properties of different components used in PEMFC. Their results also showed a dependence of thermal conductivity of these components on water content.

The thermal conductivity and resistivity values for PTL and nafion 1110 membrane found by Burheim et al. were used to estimate the degree of humidification of components constituting the system of the present work. The technique of investigating the humidification state in the membrane and the flooding of gas diffusion layers (GDL) have been tried by H.P.Drah et al. [24]. They observed a decrease in GDLs and membrane thermal resistance which favoured flooding and lowered the fuel cell performance. [22, 24]

The results discussed above have shown to be more stable horizontal plane when considering the flow of heat to be in vertical plane. By looking at the temperature difference over the PTL it becomes hard to exactly know the actual position of thermocouple leading to small uncertainties in that small temperature difference over the PTL and thus affecting the temperature difference over the membrane. At lower temperature gradients, the double standard deviation of temperature difference over PTL approaches 50 %. This can be due to huge condensation of water passing through the thermocouples in the PTL-matrices.

The temperature difference over the membrane can still be less than that measured over channels due to the same reason that it's not always that these thermocouples makes holes through the PTL.They may just make a room, and consequently increasing the heat fluxes through those areas.

The same observation regarding the difficulty in measuring the exact temperature between the electrode surface and membrane has been made by Vie et al. [16]. They encountered the same problem of sizes of thermocouples, though they did not provide much data on this issue.

After a thorough analysis on how to determine the exact temperature between the membrane electrodes, it

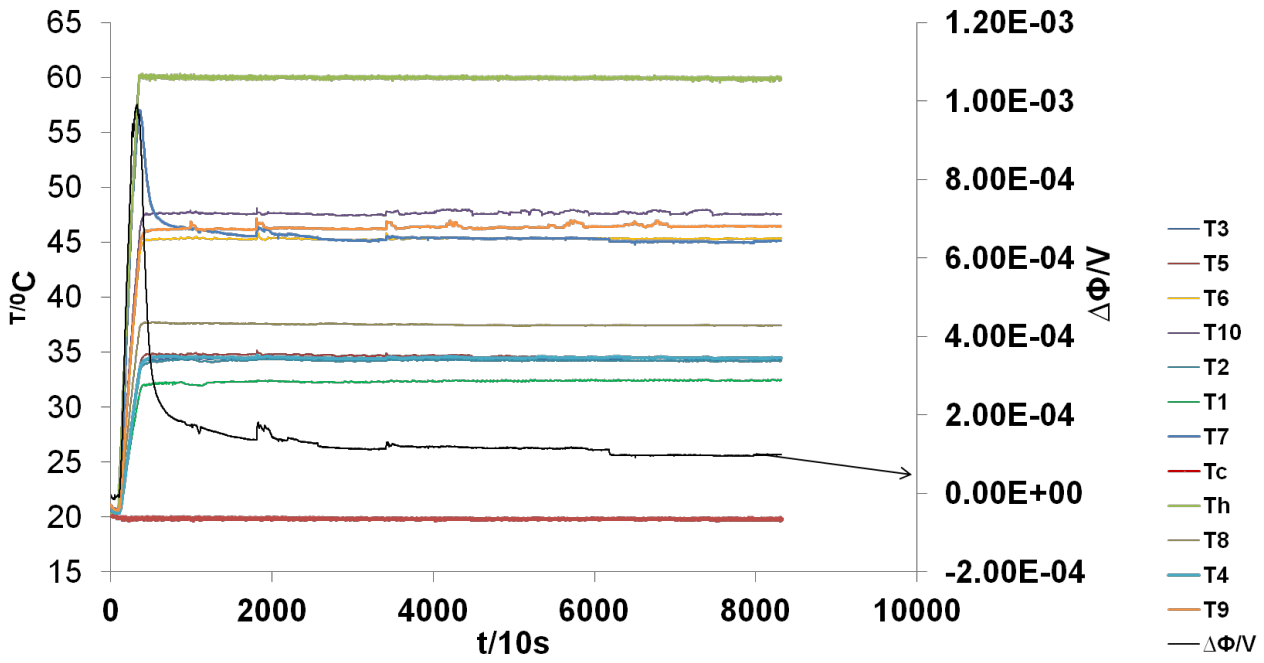

Figure 7: An arbitrary measured temperature within the same planes where the voltage is measured. The distribution of temperature in the same plane is uniform except when a thermocouple gets out of the plane. See also Table 2.

is clear that inserting thermocouples between these areas will cause more ruins on both the components and reduce the performance of the concentration cell drastically. If no other better method is available, it can be suggested to increase the carbon paper on top of PTL coated with catalytic layer to support the PTL so that it can resist on the stresses caused by thermocouples when inserted in the cell. In the same way, few thermocouples should be inserted to avoid multiple blockage of active sites to maximize the harvest of the voltage.

5.2 The voltage or electrical potential

In the previous section, 5.1.2, it was shown that the results repeated after opening the cell would increase the errors in the measured voltage due to the consequences caused by the thickness of thermocouples on the components within the cell. It was observed that the results of the measured voltages at the same operation conditions were varying very much after opening the cell and reassembling it. This made it hard to reproduce the same values after re-assembling the cell and it became difficult to determine the small variations found between the Seebeck coefficients at different pressures.
For this reason, only the results of the voltage found with 3 membranes will be presented here. This is to exclude and minimize as much as possible the errors originating from disturbances caused by manual insertion of thermocouples. This ensure that all the experiments are performed on the same physical basis. The remaining changes can now only be due to some other causes which will depend on the operation conditions (Temperature, state of water and pressure). Furthermore, in section 5.2.2 and 5.2.3, it will be shown that state of water before entering the cell after steady state has established contributes more on the fluctuations of the open circuit voltage.

Figure 8(a) show a typical potential polarization curve as function of time. The same graph shows also the temperatures of the reservoirs and local temperatures. The experiment was done under 0.05 bar. The temperature in the reservoirs were 60 and 20°C respectively. The reproducibility of voltage gave an uncertainty of around ± 5 % double standard deviation from the average. While the reproducibility deviation of temperature difference over the membrane is less than 4%.This error in temperature can be attributed to the state of water coming in the cell. Water comes in the cell as vapour and as liquid. Since the potential was measured with reference to the high temperature electrode, the electrical potential will always be more negative. [12] Figure 8(b) shows Seebeck coefficient as function of number of membrane. It follows from literature that the potential and temperature differences are the dependent on the thickness of the membrane or distance between the

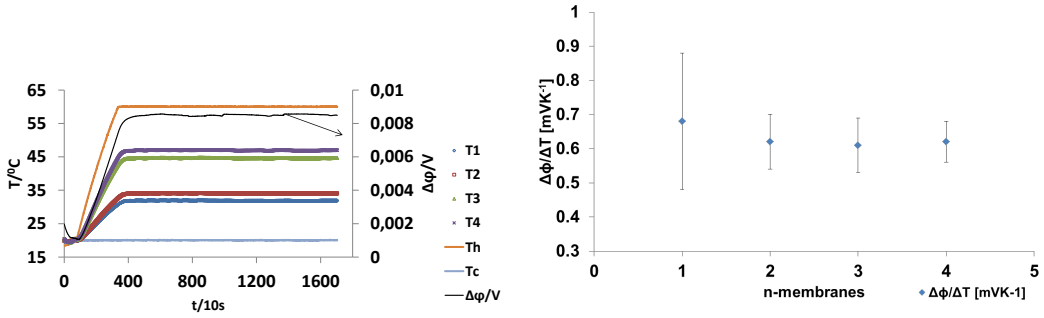

(a) A typical voltage and temperature measurement of one data.

(b) Seebeck coefficient vs nr-of membranes at 1bar and 40 °C

Figure 8: The figure (a) shows a typical voltage and temperature measurement of one data as function of time T_h and T_c were 60 and 20°C respectively in the baths. The cell was run at 1bar. Temperature in humidifier was 65°C., The figure (b) shows a function of Seebeck coefficient as function of number of membrane,n.

electrodes. When the two terms divides, the thickness or distance term cancels as shown in Eq.(30)

$$\frac{\Delta\phi}{\Delta x}/\frac{\Delta T}{\Delta x} = \frac{\Delta\phi}{\Delta T} \tag{30}$$

The error in the first data is due to probable leakages in the in the catalytic layers because the similar compression pressure was used to all the experiment. The weight of this pressure might have been high when only one membrane was used. The values are the averages of experimental values done under same physical condition and operation condition of the test facility. That's to say only data which were performed without opening the cell and repeated in the same condition were considered. It is clear that the errors have to be expected if the reasons pushed forth in section 5.1.2 are considered. Nevertheless, they become minimal as the condition of sorting data performed under same physical and operation conditions is taken into account. This is an indication which shows that the hypothetical assumption made in the theory that no heat leakage would be in the perpendicular direction to x-direction is fulfilled. See section 3.2.

5.2.1 Initial voltage

Fig. 3 shows a typical voltage measurement with temperatures. Initially, when $\Delta T_m$is zero, t is also considered zero. At these conditions the voltage varies between 0 ± 200 μV. In the present work, the initial values of voltage were not the main point of focus because the corresponding Seebeck coefficient gave no meaning due to fluctuated number of temperature difference around zero (ref. to the explanation given in section 3.4).

In fact, the initial voltage can approach zero, will not be zero due to very small currents which is caused by the active sites. The time to get the initial voltage to approach zero was found to take long time compared to the time it took to reach quasi stationary state when the temperature gradient was increased.

5.2.2 Steady state voltage

From Fig. 3 and 8(a) the voltage development with the temperature difference is shown. The voltage starts to relax at slower pace than the temperature. For smaller temperature differences, the relaxation difference between the temperature and the voltage was not noticeable. Parameters which have shown to have very big impact on the voltage magnitude and stability in addition to those discussed already in the above sections, were; the water content in the membranes and increase in ΔT_m. When the hotter half cell was subjected to a 95 °C, and the colder half cell held at 25 °C, the gas flow rate of the outlet gas appeared to increase. This can be due to dilation of materials in the cell and the increase of water activity as the temperature difference was increasing. It can also mean that the evaporation process increased as one side was heated highly. The application of very high temperatures should be done with care since they can easily lead to stretching and thus breakage of materials which are subjected to a very high temperature. If this happens, the voltage can hardly relax due to gas crossover through the materials. This can eventually lead to a very poor performance of the cell. The illustration of such case is not shown in this report though it was rejected because,after the temperature

stationary state, the voltage quasi state did not hold longer before it started behaving as it is described in this paragraph.

5.2.3 The impact of membrane thickness on the voltage

The Fig. 8(b) shows the how the thickness of membrane can help to get a more stable Seebeck coefficient. These results suggest that the thickness of the membrane will not increase the open circuit voltage but will improve the performance.
The big thickness size of membrane used in this work was obtained by compressing the bits of same membranes together. Having such condition in the cell, the state of water in different layers can be expected to be different in different layers of the membranes. This situation also can happen in other layers in the cell due to temperature gradient. The different water states in different layers could be balanced as a constant temperature difference relaxes with time.
Nevertheless, if a new state of water would come into the cell after this water equilibrium it would disturb this balance and hence perturbs the already established voltage in the cell under the existing conditions. This situation can be seen in some results of single voltages in the Appendix. In some cases the voltage found to be falling after reaching steady state and slowly tries to rise back to its true stationary state.

The main cause of the change in the state of water in the cell can be attributed to the distance between the humidifiers and the cell. The nature of the hoses which lead saturated gas into the cell could cause water to condense prior to entering the cell due to temperature difference between the humidifiers and the cell. This problem can be mitigated by implementing a metal coil hose between the humidifiers and the cell. Moreover controlling the temperature of the saturated gas right at the entrance of the cell can ensure a constant phase of water enters the cell all the time. Hence a state of water equilibrium can be achieved in different parts of cell through out the all the experiments and the reproducibility can be reached without too much struggle. By achieving this the contribution of Soret effect to thermopower can possibly be observed clearly in the cell voltage.

5.3 Seebeck coefficients

After getting knowledge of the appropriate section conditions, the right data could then be sorted, studied and compared against the literature. The appropriate selection were based on the reliability of $\Delta_{as,sc}$ i.e on the sameness of state (same water content, same pressure and temperature at the measuring points of both temperature and voltage). These conditions have been discussed and met in the previous sections.

By meeting the appropriate conditions, the thermoelectric power showed to have a dependence on the activity of the electrode reactants. It was possible,with the obtained results, to show that the thermopower was related to the activity of H_2 by the ideal gas law [9];

$$\frac{\Delta\phi}{\Delta T} = const - \frac{R}{nF} ln(P_{H_2}) \tag{31}$$

where n is the number of transferred electrons, R is the gas constant and P_{H_2} is the partial pressure of hydrogen. The Seebeck coefficients were determined from the slope of the cell potential, $\Delta\phi$ versus ΔT_m. Fig. 9(a) gives an illustration of how the relation between the $\Delta\phi$ and ΔT_mwere linear. Their slope gave 0.805 ± 0.008 mV and the variation of reproducibility of this value was of 1%. The y-intercept was about 0.03 ± 0.07. It is a sign which shows the direct dependence of the voltage with temperature difference in a thermocell.

Fig. 9(c) shows the impact of the measured temperature difference(ΔT_m) and voltage on the individual data and as group data. The results shows less error from temperature measurements on single data, but shares the contribution on the deviations between data. When looking at the individual data,(See Fig. 9(b)), one can see that the cell had reached its steady state,and water equilibrium was reached within the layers but with some negligible disturbances from different sources which can eventually be attributed in great part from water state as discussed in section 5.2.3.

It was shown in section 5.1.2 that temperature had a big contribution to changes of the magnitude of Seebeck coefficient. See the Tab. 1. While in section 5.2.2 and 5.2.3, other big sources of errors on individual measured voltage data were found to exist. By applying statistical analysis on the errors propagated into the Seebeck coefficient it can be seen that the bigger error contribution in individual Seebeck coefficients originated mostly

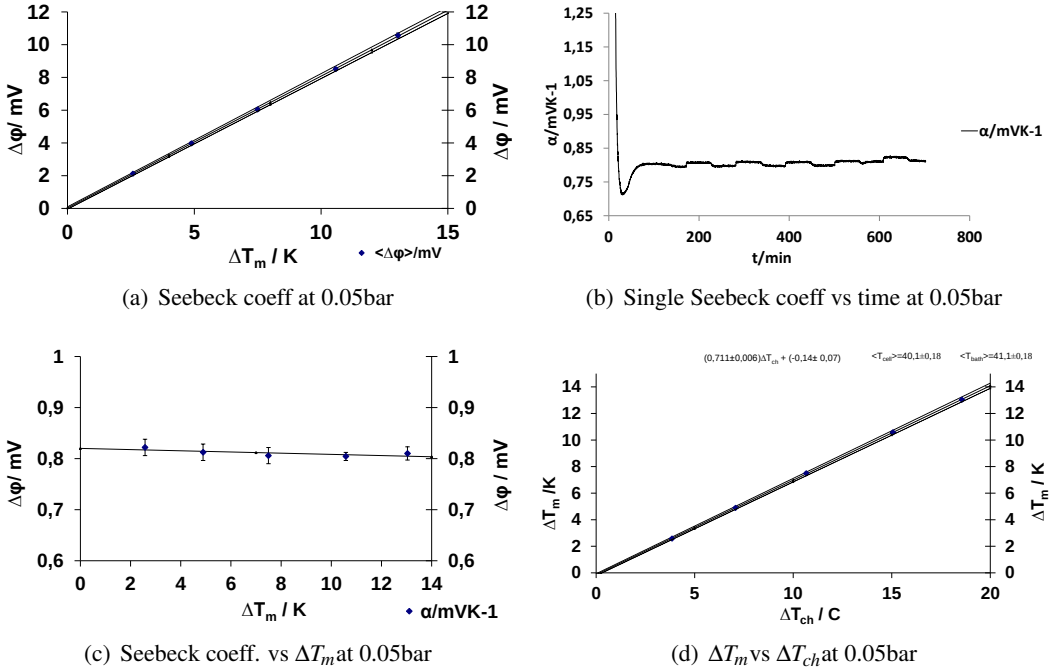

(a) Seebeck coeff at 0.05bar

(b) Single Seebeck coeff vs time at 0.05bar

(c) Seebeck coeff. vs ΔT_mat 0.05bar

(d) ΔT_mvs ΔT_{ch}at 0.05bar

Figure 9: The figures (a), (b), (c) and (d) show the typical Seebeck coefficient results obtained at the average temperature of 40°C at 0.05bar, the Seebeck coeff.vs time, the typical stable individual seebeck coeff varying with $\Delta T_m$and the f_{ratio} from ΔT_mvs ΔT_{ch}respectively.

from the error in the measured voltage. The statistical analysis could be easily achieved by taking two arbitrary data (one voltage data measured at an arbitrary temperature difference) and then apply the analysis of variance and dispersion of errors on them . The Eqs.27 and 28 were used to achieve this analysis. From this point of view, it was found that the propagation of errors between the groups was less than the errors within the groups. That means, the errors from temperature measurements affected less than voltage the standard deviation of the individual Seebeck coefficient. But they had a share in the variations between the Seebeck coefficients. See section 5.1.2 to get more insight on the contribution of temperature difference on the variations of Seebeck coefficients.

The results conducted at the average temperature of 40 °C at 5 different pressures are presented in this section. The experiments conducted at the same average temperature are the ones discussed in this work. Due to time limitation, only the experiments done at 40°C cell average temperature are discussed. The experiments done at 60°C were also attempted but were not tried at other pressures. Due to some technical problems encountered during work, it was important to prioritise the condition which had already show some promising trends. The potential of the hotter electrode was more positive and was increasing with increase in temperature difference, but not average temperature. This means the hotter electrode was a absorbing heat and delivering it to the cooler side to produce more electrons. The heat produced/or sunk in this electrode was transported to the cooler side by cations and water molecules. At equilibrium, one should expect some transported entropies from the colder side to the hotter side, but this will be of small magnitude compared to that transported to the colder side, as it was clarified by Agar, when a concentration cell has univalent ions of opposite signs in the electrolyte. In the case of this experiment, one would expect instead, the transport of water from colder side to the hotter side by the effect so-called Soret effect, or thermo-diffusion effect. This effect would contribute in very insignificant amount to the produced voltage, since it takes days before it reaches steady state, and it's in the order of (10^{-2}) compared to the produced voltage, which is in the range of fluctuation of the observable voltage. So, this makes the work easier for estimation of remaining parameters.

Another assumption to consider is to minimize thermopower contribution from thermocouples. Since Pt was used to measure the potential directly at the interface, the thermopower arising from this can be neglected also. The remaining parameter to find with be just the transported entropy which is related to the entropy transported by the migration of ions and electrons. The average temperature and pressure in the reservoirs and in the cell are held constant throughout the measurement of the Seebeck so that the resulting power can be used to calculate Peltier coefficient. This is to make sure that net increment of entropy of junction region is zero for better comparison in the system. The fig 10 shows how the voltage was varying with temperature difference

but not with the average temperature. Thi happened both when increasing the temperature difference and when this latter is decreased. This confirms the reversibility of thermal dependent e.m.f. The figure shows though the temperature was increased on both sides, it was not a guarantee for increasing the voltage or thermopower.

There must be proportional increase in the voltage with respect to temperature difference. A more rapid temperature gradient than potential gradient, will result into a delay in the steady state of the voltage compared to temperature difference. The cause for such occurrence can be many and were discussed in previous sections.

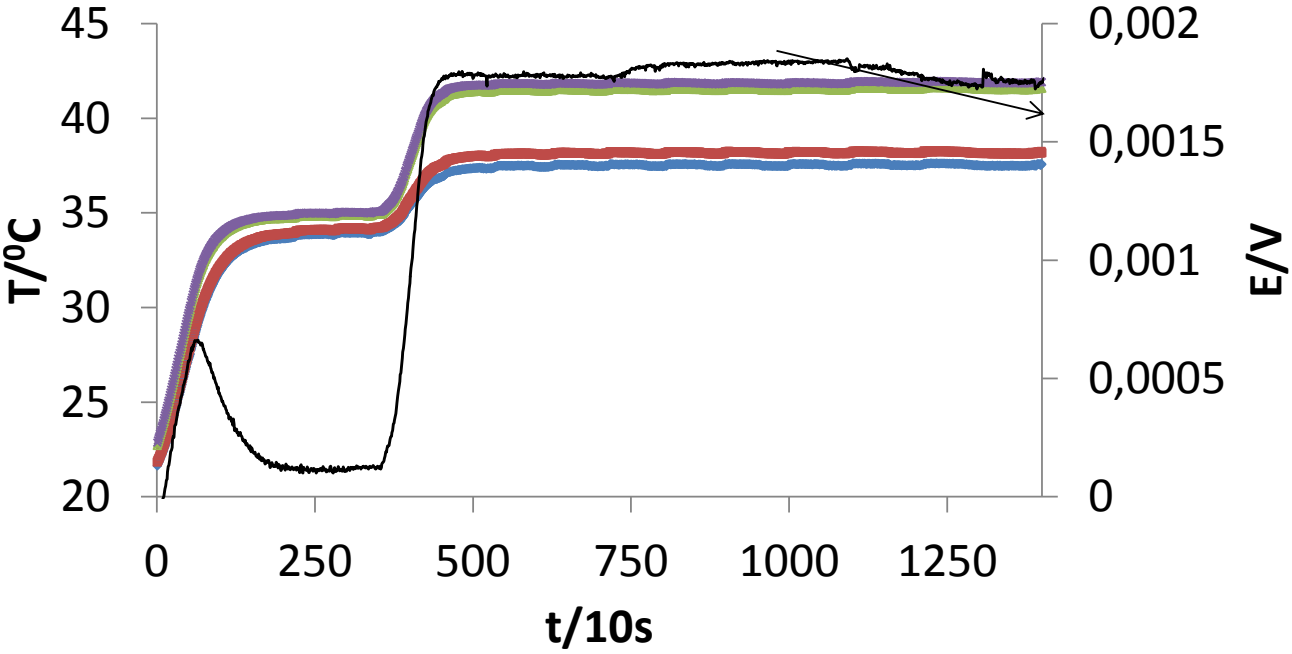

Figure 10: The measured voltage and the corresponding temperature difference. The average cell temperature was 40°C with temperature difference over the membrane of 3.369 ± 0.045. The voltage was of 1.80 ± 0.069 at an average temperature of 39.79 ± 0.083°C. The thicker lines are the temperatures at different locations in the cell as shown in the Fig 2 , where the higher temperatures are measured at the point ④ and ① and the rest corresponds to the other numbers in the Fig 2.

The cause for this delay can be due to a slow response of molecule adsorption on the temperature difference force. As a matter of fact, though steady state may have already established on some local places in the cell, such as in the interfaces, that may not be the case within the membrane due to its thicker size than other parts of the cell used. Also, in case this could take very long time, the voltage could start to drop down and re-establish itself later on. Otherwise, one had to reduce the temperature gradient and shoot it again up to push the reaction or quick flow of energy distribution within cell.

Several other causes for voltage drop in a thermocell have already been discussed in previous sections. The slopes fell voltbetween 0.51 mV/K and 1.6 mV/K for experiment of hydrogen electrode with for all attempted 6 partial pressures(1.5,1,0.75,0.5,0.25 and 0.05bar).

5.3.1 Partial pressure dependence of Seebeck coefficient

In this work 5 different pressures have been attempted to confirm the relation of thermopower with the electrode reactants and the Fig 11 shows this dependence.The results confirms the validity of the results of this work since the coefficient found lies near $\frac{R}{nF}$. The hydrogen partial pressures used were 1, 0.75, 0.5,0.25 and 0.005bar. The results have shown to be less errors in the Seebeck coefficient at low hydrogen partial pressures and partially reproducible on high pressures. This is indeed in agreement with previous works which investigated on the thermoelectric power of concentration cells [15, 9, 14]. They found that it was easier to measure the seebeck of dilute solutions than that of high concentration. This can be explained by the fact that the transported entropy of any solute is originally determined by partial molar entropy which include a deviation term from ideal behaviour. This term, disappears as the main force in dilute solution is ionic interaction which is not the case in a more concentrated solution. This calls for more attention to other factors which may arise such as the temperature in the membrane and the water content in the membranes.

From Fig.11 it can be seen that as the pressure was increasing, the replication of the experiment was becoming harder and harder. In fact, the case of this work had much water molecule per sufonic group in the

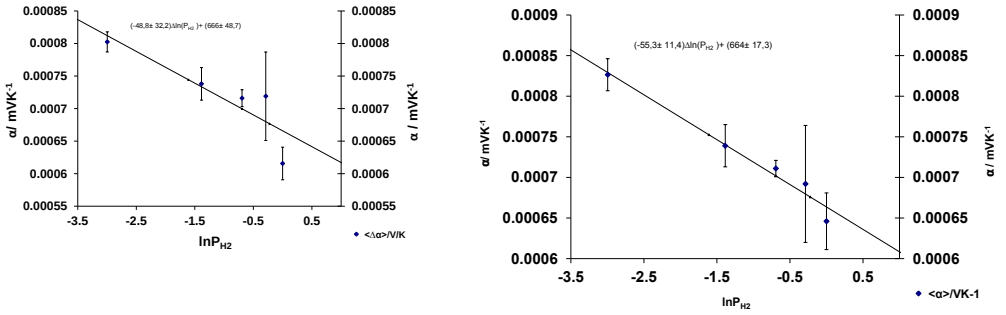

(a) Seebeck coeff vs $mathrmH_2$ activity

(b) Seebeck coeff y-intercepts like in Fig. (c) vs H_2 activity. The values of

Figure 11: The figures (a), and (b) Show the linear dependence of $\frac{\Delta\phi}{\Delta T_m}$. Fig.(a) was obtained from the direct measured seebeck coefficients and gave a slope value of $-48.8 \pm 32.2\,\mu\text{V/K}$. The coefficient was The results of Fig.(b) were obtained from the seebeck coeff taken from y-intercepts of Seeb coeff vs ΔT_msuch as in (c) and gave a slope value of $-55.3 \pm 11.4\,\mu\text{V/K}$

Nafion. At high partial pressures one can expect the movement of hydrogen to increase in such a way they easily interact with the polar water molecule and can even interact with near molecules a more ordered environment resulting in decreasing transported entropy. On the other hand for a more dilute solution, where there is a long range interactions, the proton will easily create temporary bonds with hydronium ions and easily break them resulting in a kind of disordered intermixing of ionic groups in the inter-phase between the fluoroether ligand and the fluorocarbon matrix [27, 28, 28]. The values from the results in Fig. 11 had very big errors of almost higher than 50 % the size. The causes for this originate more specifically in both the above arguments on transported entropy if hydrogen at high activity and partly on the statistical analysis of measured voltage.

5.3.2 Temperature dependence of Seebeck coefficient

Two experiments were attempted with a cell average temperature of 60°C and 1 bar and 1.5 bar respectively. The Seebeck coefficients still lie in the same error interval of those with lower average temperatures. At 1 bar, the slope gave thermoelectric power of the size 0.711 ± 0.0197 mV/K with an intercept of -0.120 ± 0.326 mV/K. At 1.5 bar, the Seebeck coefficient was 0.673 ± 0.024 mV/K. See fig. 12

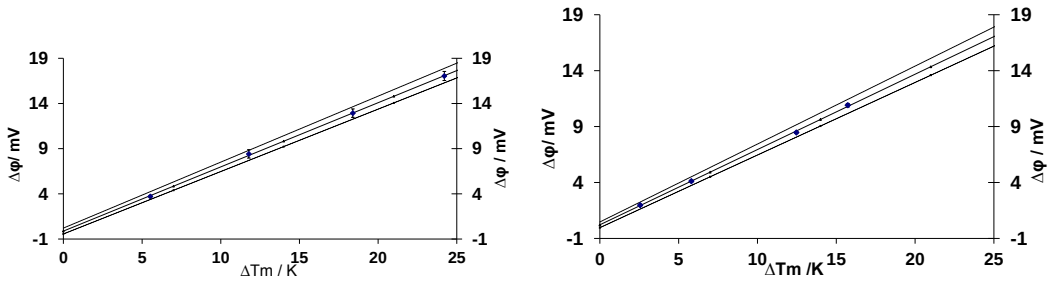

(a) 60°C at 1bar

(b) 60°C at 1bar

Figure 12: The figures (a), and (a) Show the results obtained from 60 °C at 1 and 1.5 bar respectively. These results do not confirm a dependence of thermopower on temperature. Their corresponding slopes are 0.711 ± 0.0197 and 0.673 ± 0.024 respectively.

Indeed, the Seebeck coefficient values found here, were not far from those found in the literatures. Different investigators have shown different values of Seebeck of H_2 - electrode from different systems. The reason for this change for most of them lies in the fact that the transported entropy of hydrogen changes with environment in which it is found.

Reproducible values found in this work have spanned through almost all those values though working in the very same system. The reason for this variety was attributed to the degree of damage inflicted by thermocouples on components in the cell and to the state of water into the cell. The Seebeck coefficients found in here ranged from 0.56 to 1.2 mV/K.

Some electrical current was drawn, but they were not enough to base some conclusions on them. Nevertheless, they showed a trend of decreasing voltage as the current increased. Which is a good indication of performance of the cell as working cell.

6 Conclusion

The coefficient of Thermoelectric power of hydrogen electrode as function of partial pressure has shown to be negative in accordance with the negative sign of state function of entropy with a deviation of almost half its size. The value found was $-48.8 \pm 32.2 \mu V/K$. The intercept was found to be about $666 \pm 48.7 \mu V/K$. This value of intercept can be used to determine the Peltier coefficient. The All the Seebeck coefficients were measured positive with reference to the hot electrode. On the other hand, this power is produced on the cost of absorbing the heat from the environment(heat reservoir). If this is related to electrolysis devices, this means more care should be taken on the hydrogen electrode which has an endothermic reaction to avoid the freezing of the anode electrode. In the case of fuel cell, this will mean that extra care should be taken on both Hydrogen and Oxygen electrode, since all the adsorbed heat are thrown to the other side of where reduction occurs. These heats have been defined as Peltier heats of single electrodes. Good knowledge of the magnitude of these heats will save the life of the expensive materials in fuel cell and will improve the design of thermocells which can in turn help the efficiency improvement of those cells. The temperature profile of the hydrogen electrode cell was analysed. The causes for drop in voltage were properly explained.

7 Future Plan

Based on the experience with the cell used the Physical Chemistry Lab, the writer of this paper would suggest few more things to be done so that the complete reliability and improvement the results found in this work can be reached. Five things can be done to improve the results found in this work, and thus final values of transported entropies of hydrogen can be found with less errors:

- Use of thinner thermocouples such as thin foil carefully inserted in the gas channels to avoid being broken when two half cells are compressed together. The thinner they are the less they will make room in the PTL.
- There should be tried to increase the thickness of PTL rather than increasing only the membrane thickness. The disadvantage of using thicker PLT can be the flooding, but, this can be neglected. As long as the uniform state of water is flowing into the cell with a constant temperature gradient we found that the performance was stable.
- It would be interesting to repeat the results performed with 3 membranes before attempting the other number of membranes to confirm the reliability of the results of this work. This can give a good reference of results against which other results can be compared in future works.
- Three to four more pressures between 0.05 and 0.25bar should be tried to reduce the errors in the pressure dependence Seebeck coefficients. Pressures such as 0.10, 0.15, and 0.20 bar can be tried. Or between 0.25 and 50bar.

References

[1] M. Helbæk and S. Kjelstrup. *Fysikalsk kjemi*. Fagbokforlaget Vigmostad & Bjørke AS, 2006.

[2] O. Burheim, P. J. S. Vie, J. G. Pharoah, S. Møller-Holst, and S. Kjelstrup. Calculation of reversible electrode heats in PEMFC. *Electrochimica Acta.*, 56:3248–3257, 2011.

[3] Y. Ito, H. Kaiya, S. Yoshizawa, S. Kjelstrup Ratkje, and T. Førland. Electrode heat balances of electrochemical cells: Application to water electrolysis. *J.Electrochem.Soc.*, 111:111–123, 1984.

[4] Dick Bedeau and Signe Kjeltrup. The dissipated Energy of Electrode Surfaces:Temperature Jumps from Coupled Transport Processes. *J.Electrochem.Soc.*, 143:767–779, 1996.

[5] S. Kjelstrup and D. Bedeaux. *Non-Equilibrium Thermodynamics of Heterogeneous Systems*. World Scientific Publishing Co. Pte. Ltd.and 5Toh Tuck Link, Singapore 596224, 2008.

[6] Signe Kjeltrup and Audun Røsjorde. Local and Total Entropy production and Heat and water fluxes in One-Dimensional PEMFC. *J.Phys.Chem*, 109:9020–9033, 2005.

[7] S. Kjelstrup, T. Førland, and K. S. Førland. *Irreversible Thermodynamics theory and Applications*. Tapir Trykkeri,Trondheim, 2001.

[8] S. Kjelstrup, D. Bedeaux, E. Johannessen, and J. Gross. *Non-Equilibrium Thermodynamics for Engineers*. Tapir Trykkeri, Trondheim, 2010.

[9] J. N. Agar. *Chap.02,Advances in Electrochemistry and Electrochemical Engineering*. John Wiley & Sons, USA, 1963.

[10] Soowhan Kim and M. M. Mench. Investigation of temperature-Driven water Transport in Polymer Electrolyte Fuel Cell:Phase-Change-Induced Flow. *Journal of Electrochemical Society.*, 156:B353–B362, 2009.

[11] Soowhan Kim and M. M. Mench. Investigation of temperature-Driven water Transport in Polymer Electrolyte Fuel Cell:Thermo-osmosis in membrane. *Journal of Electrochemical Society.*, 329:113–120, 2009.

[12] M. Kamata, Y. Ito, and J. Oishi. Single Electrode Peltier Heat of Hydrogen Electrode in NaOH solutions. *Electrochem.Acta.*, 33:359–363, 1988.

[13] M. Bonetti, S. Nakame, M. Roger, and P. Guenoun. Huge Seebeck coefficient in nonaqueous electrolytes. *J.Chem.Phys.*, 134:114513–1–114513–8, 2011.

[14] J. N. Agar and W. G. Breck. Thermal Diffusion in Non-Isothermal Cellsl. *RSC Publishing*, 53:167–178, 1956.

[15] H. H. V. Tyrrell and G. L. Hollis. Thermal Diffusion Potentials in nonisothermal electrolytic systems, Part1. *Trans.Faraday Soc.*, 45:411–423, 1949.

[16] Preben J. S. Vie and Signe Kjelstrup. Thermalconductivities from temperature profiles in PEFC. *Electrochimica Acta*, 49:1069–1077, 2004.

[17] Preben J.S. Vie. *Characterisation and Optimisation of the Polymer Electrolyte Fuel Cell*. NTNU,Trondheim, May 2002.

[18] G. Vasu, A. K. Tangirala, B Viswanathan, and K. S. Dhathathreyan. Continuous bubble humidification and control of relative humidity of H_2 for a PEMFC system. *International Journal of Hydrogen Energy.*, 33:4640–4648, 2008.

[19] Odne S. Burheim. *Thermal Signature and Thermal Conductivities of PEMFCs*. NTNU,Trondheim, 2009.

[20] E. D. Eastman. Thermodynamics of non-isothermal systems. *J.Am.Chem.Soc.*, 48:1482–1493, 1926.

[21] E. F. Medici and J. S. Allen. The Effect of Morphological and wetting properties of PTL. *J.Electrochem.Soc.*, 157:B1505–B1514, 2010.

[22] Shuo-Jen Lee, Kung-Ting Yang, Yu-Ming Lee, and Chi-Yuan Lee. Resistive Properties of Proton Exchange Membrane Fuel Cells With Stainless Steel Bipolar Plates. *Journal of Fuel Cell Science and Technology.*, 7:041004–1, 2010.

[23] Se-Kyu Park, Eun Ae Cho, and In-Hwan Oh. Characteristics of Membrane Humidifiers for Polymer Electrolyte Membrane Fuel Cells. *Korean J.Chem.Eng.*, 22:887–881, 2005.

[24] H. P. Dhar and S. K. Chaudhur. Measurements of fuel cellinternal resistances for the detection of electrode flooding. *J.Solid State Electrochem*, 13:999–1002, 2009.

[25] O. E. Herrera, D. P. Wilkinson, and W. Merida. Anode and cathode overpotentials and temperature profiles in PEMFC. *Journal of Power Source.*, 198:132–142, 2012.

[26] O. Burheim, P. J. S. Vie, J. G. Pharoah, and S. Kjelstrup. Ex situ measurements of through-plane thermal conductivities in a polymer electrolyte fuel cell. *Journal of Power Sources.*, 195:249–256, 2010.

[27] Arun Venkatnathan, Ram Devanathan, and Michel Dupuis. Atomistic Simulations of Hydrated Nafion and Temperature Effects on Hydronium Ion Mobility. *American Chemical Society.*, 111:7234–7244, 2007.

[28] P. J. Reucroft, D. Rivin, and N. S. Schneider. Thermodynamics of water Nafion-Vapor interactions.I.Water vapor. *polymer*, 43:5157–5161, 2002.

8 APPENDIX

Data for the experiments done at 0,05 bar with 3 Nafion-1110 membranes at a flaw rate of 0,02l/min.

Parallell	α /mVK^{-1}	f_{ratio}	$<T_{bath}>^0$C	$<T_{cell}>/^0$C	$\Delta\varphi$/mV	ΔT_m/K	ΔT_{ch}/K	$\alpha(\omega)$/mVK^{-1}
1	0,805±0,008	0,71±0,01	41,7±0,1	40,4±0,1	2,12±0,04	2,58±0,03	3,85±0,03	0,822±0,016
			41,2±0,1	40,1±0,1	4,0±0,1	4,89±0,04	7,07±0,07	0,812±0,016
			41,2±0,19	40,1±0,1	6,0±0,1	7,50±0,08	10,66±0,05	0,806±0,016
			40,03±0,17	39,4±0,1	8,5±0,1	10,58±0,04	15,06±0,06	0,804±0,008
			40,0±0,14	39,7±0,1	10,56±0,15	13,04±0,06	18,6±0,1	0,810±0,013
2	0,800± 0,030	0,71±0,01	41,66±0,16	40,4±0,1	2,05±0,07	2,53±0,03	3,78±0,03	0,81±0,03
			41,10±0,13	40,13±0,04	4,01±0,04	4,76±0,03	6,89±0,03	0,84±0,01
			41,10±0,13	40,3±0,1	6,2±0,1	7,36±0,06	10,6±0,1	0,84±0,01
			40,01±0,12	39,5±0,1	8,43±0,15	10,30±0,03	14,89±0,04	0,819±0,015
			40,01±0,4	39,9±0,2	10,16±0,19	12,65±0,15	18,31±0,17	0,80±0,01

Data for the experiment done at 0,25 bar with 3 Nafion-1110 membranes at a flaw rate of 0,02l/min.

Parallell	α /mVK^{-1}	f_{ratio}	$<T_{bath}>^0$C	$<T_{cell}>/^0$C	$\Delta\varphi$/mV	ΔT_m/K	ΔT_{ch}/K	$\alpha(\omega)$/mVK^{-1}
1	0,74±0,03	0,707±0,012	41,83±0,10	40,51±0,07	1,84±0,04	2,56±0,03	3,80±0,03	0,730±0,008
			41,13±0,11	40,07±0,06	3,52±0,03	4,75±0,03	6,89±0,05	0,742±0,008
			41,12±0,17	40,26±0,06	5,53±0,09	7,31±0,03	10,53±0,06	0,756±0,011
			40,01±0,19	39,5±0,1	7,9±0,3	10,45±0,13	15,1±0,2	0,751±0,026
			39,96±0,13	39,6±0,1	9,6±0,4	13,07±0,05	18,56±0,08	0,732±0,033
2		±	±	±	±	±	±	±
			±	±	±	±	±	±
			±	±	±	±	±	±
			±	±	±	±	±	±
			±	±	±	±	±	±

Data for the experiment done at 0,5 bar using 3Nafion-1110 membranes at a flow rate of 0,02l/min.

Parallell	α /mVK^{-1}	f_{ratio}	$<T_{bath}>^0$C	$<T_{cell}>/^0$C	$\Delta\varphi$/mV	ΔT_m/K	ΔT_{ch}/K	$\alpha(\omega)$/mVK^{-1}
1	0,716± 0,013	0,706±0,005	41,77±0,16	40,53±0,05	1,85±0,05	2,60±0,03	3,87±0,04	0,712±0,020
			41,11±0,13	40,05±0,06	3,43±0,05	4,82±0,02	6,95±0,03	0,712±0,011
			41,22±0,13	40,44±0,07	5,30±0,05	7,42±0,04	10,63±0,04	0,714±0,008
			39,91±0,19	39,42±0,07	7,6±0,2	10,56±0,04	15,12±0,06	0,723±0,022
			39,99±0,15	39,9±0,2	9,2±0,7	12,9±0,3	18,5±0,4	0,711±0,041
2		±	±	±	±	±	±	±
			±	±	±	±	±	±
			±	±	±	±	±	±